UNSTEADY WALL PRESSURE MEASUREMENTS ON A FULL SCALE FLEXIBLE CHIMNEY SUBJECT TO NATURAL WIND

Yacine Manal
LadHyX, CNRS-Ecole polytechnique, Palaiseau, France & ENS Paris-Saclay, France

Pascal Hémon
LadHyX, CNRS-Ecole polytechnique, Palaiseau, France

ABSTRACT

A full scale flexible prototype chimney is erected on a natural site in order to study its excitation by wind, especially by the alternate vortex shedding. For the first time, unsteady wall pressure measurements are performed on the chimney. This experiment combines the two features that cannot be reproduced simultaneously in wind tunnel: a high Reynolds number and a turbulent boundary layer.

Preliminary results are presented, showing notably that the pressure distribution looks like the one measured in wind tunnel in supercritical conditions, with an additional turbulent noisy component.

1. INTRODUCTION

Vertical slender flexible structures are subject to wind-induced vibrations involving complex inflow conditions due to the atmospheric boundary layer. Especially structures with circular, or mostly circular, shapes, such as chimneys, stacks and launch vehicles, are responsive to alternate vortex shedding. However, there are a number of difficulties for studying such a phenomenon while respecting the natural wind characteristics such as the velocity gradient and the turbulence parameters. Moreover, wind tunnel tests in such cases are performed on scaled models, which do not respect the Reynolds similarity and introduce an additional difficulty then. For instance, numbers of authors add roughness elements on the surface model in order to simulate the high Reynolds number flow (Barré & Barnaud 1995) while the technique is not reliable (Ellingsen et al. 2022b).

Despite their interest, there are very few field studies of vortex-induced vibrations of chimneys that can serve as validation test cases for the prediction model, such as (Basu & Vickery 1983, Vickery & Basu 1983). In (Sageau 1978) and (Christensen et al. 1978) some wall pressure measurements were performed on some existing chimneys. An interesting experiment was presented in (Galemann & Ruscheweh 1992 ; Ruscheweh & Galemann 1996) where an experimental steel chimney of 28 m was equipped with a number of sensors, including wall pressure.

In all these experiments, only the time-averaged wall pressures were measured while unsteady data would be useful in the context of vortex shedding understanding in real wind conditions.

In 2018 a project was started under a partnership including the company Beirens, the CNES, the CSTB and LadHyX. One of its components was the erection of an experimental chimney on an observation site for which first results were presented in (Ellingsen et al. 2022a). The goal of the current paper is to present the preliminary results of the wall pressure measurements performed during a short term campaign in July 2021.

2. FIELD TEST PLATFORM

The observation site is located in Bouin (85, Département of Vendée) in the western part of France at about 2 km from the Atlantic seashore. The environment is a marsh which makes the relief very flat over a distance greater than 2 km around, as it can be seen in the Figures 1 and 2.

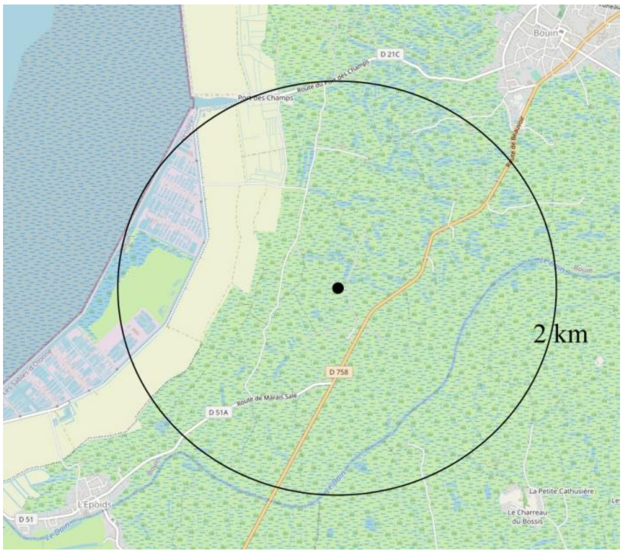

Figure 1. Map of the chimney site

2.1. The experimental chimney

The chimney is a steel tube with 35.5 m high and an external diameter of 1 m in the lower part from 0 to 12 m and 2 m in the upper part above 15 m. From 12 to 15 m the diameter linearly increases from 1 to 2 m (see Figure 3). It is clamped at the bottom in a concrete mass.

The purpose of this particular shape is to obtain a chimney with a low Scruton number and a first bending mode at a low frequency in order to get a lock-in with alternate vortex shedding at moderate winds.

Figure 2. Photos of the chimney and the wind mast

The total mass of the chimney is 11276 kg including all additional masses necessary for mounting, maintenance and human access. The equivalent mass m_e per unit of height is computed using the first mode shape $\psi(z)$ which is obtained via a structural analysis (Simiu & Scanlan 1978; Eurocode 2005):

$$m_e = \frac{\int_0^h \psi(z)^2 m(z) dz}{\int_0^h \psi(z)^2 dz} \qquad \#(1)$$

A value of $m_e = 322.6$ kg/m was obtained.

The Scruton number reads:

$$Sc = \frac{4\pi\eta\, m_e}{\rho d^2} \qquad \#(2)$$

The reduced structural damping referred to critical damping η was measured in situ in two normal directions via the records of the chimney motion after a manual release. It was found that $\eta = 0.185 \pm 0.005$ %. Using the air density $\rho = 1.225$ kg/m^3 and the upper diameter $d = 2$ m of the chimney, the Scruton number is $Sc = 1.53$.

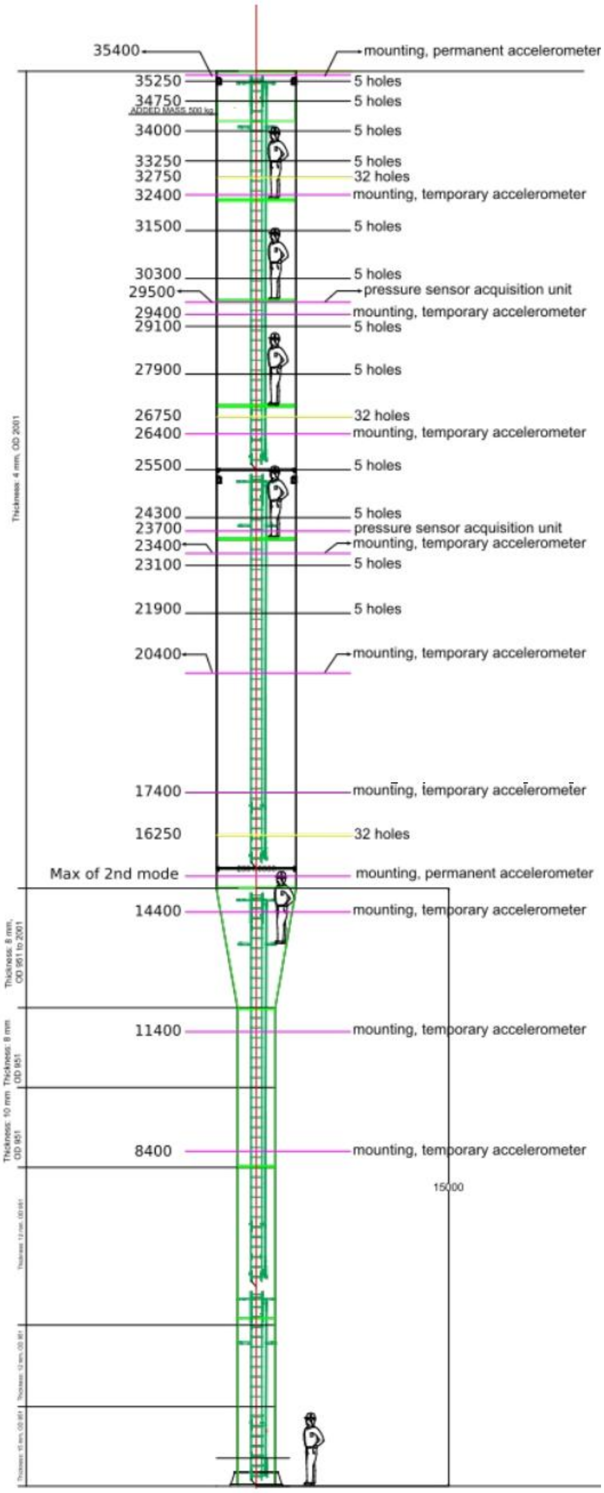

Figure 3. Detailed design of the chimney

The first bending frequency was measured in the same way as the reduced damping. It was found that $f = 0.868 \pm 0.001$ Hz.

The Strouhal number reads:

$$St = \frac{f\,d}{\overline{U}} \qquad \#(3)$$

It is supposed to be 0.18 in (Eurocode 2005) but potentially 0.21 (Ellingsen et al. 2022). Therefore the lock-in mean velocity is expected to be in the range $\overline{U}_c = 8.3 - 9.6$ m/s, a relatively moderate wind frequently observed on the site.

Associated to the low Scruton number mentioned above, high oscillation amplitudes at lock-in are expected.

2.2. Wind mast

A mast of 40 meters high is erected at the distance 55 meters from the chimney in the west direction. It is equipped with 4 anemometers at 10 (cup) , 18 (propeller), 25 (3D sonic) and 35 (propeller) meters of height. Three wind vanes complement the cup and the propeller anemometers. All these sensors are shifted from the mast axis by 1.5 m in order to limit the interactions.

Figure 4. Photo of the wind mast

The cup anemometer at 10 m has an accuracy of ±0.1 m/s, while the propellers at 18 and 35 m have and accuracy of ±0.3 m/s. The vanes provide the wind direction with an accuracy of ±3°.

The 3D sonic anemometer has better characteristics, with an accuracy of ±0.05 m/s and ±2°. It continuously records the wind velocity components at the sampling frequency of 5 Hz.

The 3 others anemometers record only statistical values (mean, RMS, maxima) of the velocity modulus and its direction in degree, referred to magnetic North, over sequences of 10 minutes.

2.3. Chimney measurement systems

Four single component accelerometers are mounted for the chimney motion measurement (type PCB 3741). They can measure in the frequency range [0-70 Hz] up to ±2 g with an accuracy better than ±0.04 g. Accelerometers #1 and #2 are fixed at 20.4 meters of height and #3 and #4 at the top, ie 35.5 meters. The directions of measurements are 45° (North-East) for accelerometers #1 and #3, and 315° (North-West) for #2 and #4. The record is continuous with a sampling frequency of 16 Hz.

Synchronized wall pressure measurements are performed by using 32-channel pressure scanners (32HD ESP pressure scanners from Pressure Systems Inc.) with multiplex frequency of 70 kHz. The global accuracy is about ±1 Pa, but difficulties in setting the zero value (the no wind response of the sensor) lead to much higher errors on the mean component. The records have a sampling frequency of 20 Hz and stored in sequences of 10 minutes long. A number of taps have been mounted (see Figure 3) but the most interesting ones are the 32 taps around the chimney at 26.75 meters of height. They are uniformly distributed around the circumference and spaced by 11.25° of the azimuth angle.

3. WIND CHARACTERISTICS

Due to the instrumentation complexity and the necessity of having a proper weather, notably without rain, observation and measurements of the wall pressures occurred during two days, July 19-20 2021. Some interesting events have occurred during these two days with a mean speed around 8-10 m/s and a wind coming from North-East, typically 50-70° referred to magnetic North.

Finally, four sequences have been selected for detailed processing and investigation. The two first from July the 19^{th} are without motion of the chimney, while the two others from July the 20^{th} are recorded during chimney oscillations. These four atmospheric boundary layers (ABL) are shown in Figure 5 where the mean velocity and the turbulence intensity are presented versus altitude. They are compared with the Eurocode profiles for the roughness type II which is supposed to apply to the present site.

In such case, the mean velocity is given by

$$\overline{U}(z) = 0.19\ \overline{U}(10)\ ln\left(\frac{z}{z_0}\right) \qquad \#(4)$$

and the turbulence intensity by

$$I(z) = 1/\ ln\left(\frac{z}{z_0}\right) \qquad \#(5)$$

where the roughness height z_0 is 0.05 m (Eurocode 2005). One should note here that the mean speed at 10 m high is the reference speed for the type II roughness, so that every velocity profile should go through that point.

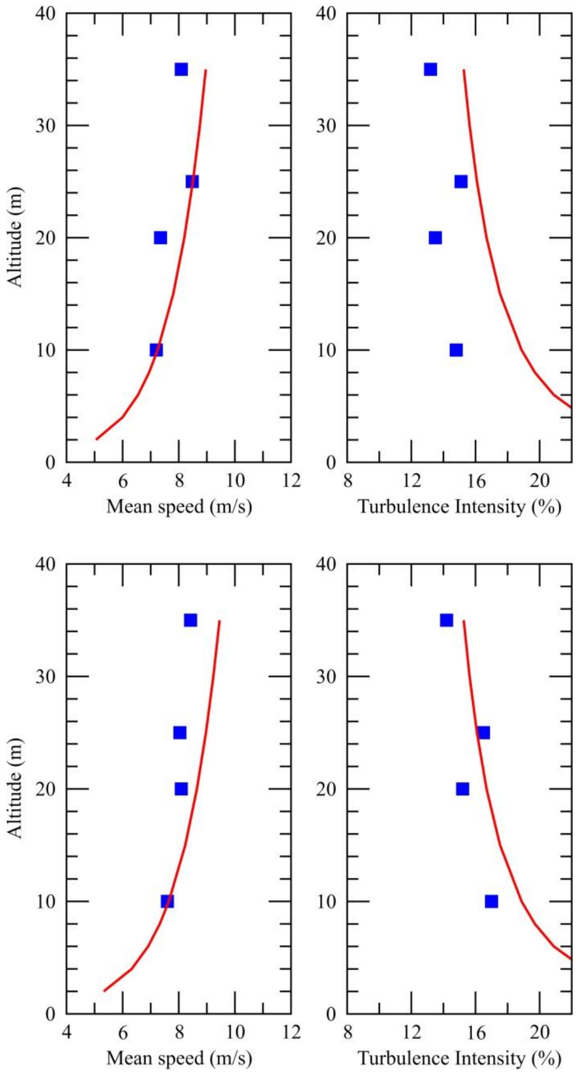

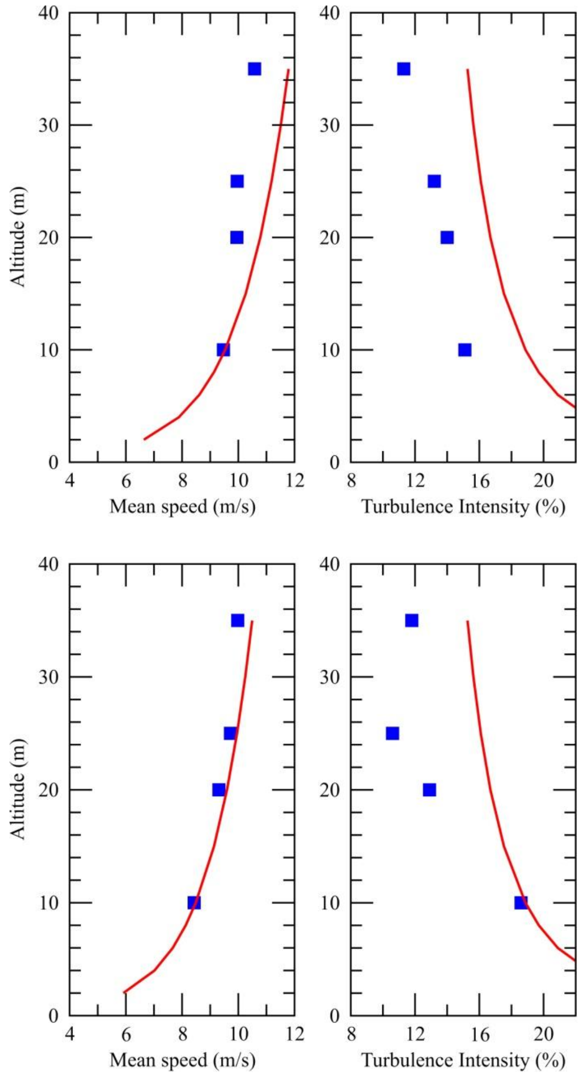

Figure 5. Measured ABL (blue square) compared with Eurocode type II ABL (red line, following Eq. 5 & 6) for four sequences; top to bottom: July 19th, 4:00 PM & 4:10 PM, and July 20th, 12:40 PM & 12:50 PM

By looking at Figure 5, it appears that, while the mean velocity gradient follows more or less well the Eurocode profile, the measured turbulence intensity is lower than the one furnished by Eurocode, excepted in one case, July 19th at 4:10 PM. Especially the last sequence presents a very low measured turbulence (10.5 % at 25 m), far from the value which is expected by the standards (16 %). Up to now, no explanation has been found to explain that behavior.

Note that the sonic anemometer located at the altitude of 25 m is supposed to be more accurate for the turbulence measurement, by comparison with the other cup or propeller anemometers that have an inertial effect.

The power spectral density (PSD) of the longitudinal velocity is computed thanks to the time records furnished by the sonic anemometer. It can be compared to the Von Karman spectrum $S_u(f)$ which reads (Simiu & Scanlan, 1978):

$$\frac{S_u(f)}{\sigma_u^2} = \frac{4\, L_u}{\bar{U}\left(1 + 70.7\left(\frac{f\, L_u}{\bar{U}}\right)^2\right)^{5/6}} \qquad \#(6)$$

where σ_u is the standard deviation of the velocity, f the frequency and L_u the integral scale of turbulence of the longitudinal component. The latter is determined by finding the best fit of the Von Karman model $\#(6)$ with the measured PSD, as shown in Figures 6 & 7 where $S_u(f)$ is normalized with σ_u^2 as in Eq. (6).

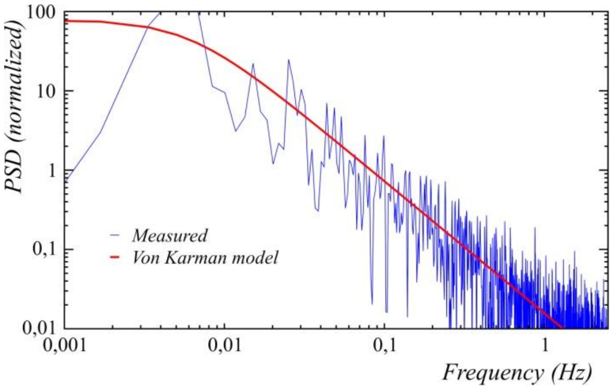

Figure 6. PSD of longitudinal velocity at 25 m, $\bar{U} = 8.49\, m/s, \sigma_u = 1.28\, m/s,\ L_u = 168\, m$ Direction 67°MN, July 19th, 4:00 PM.

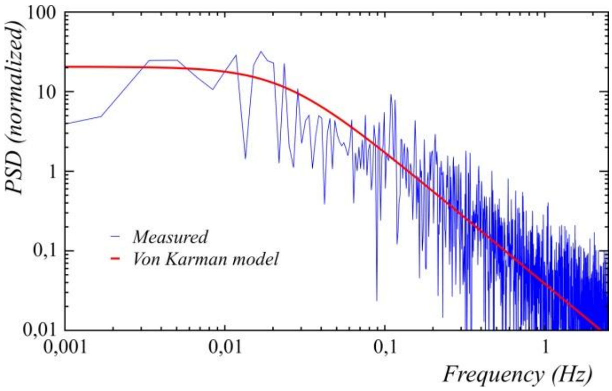

Figure 7. PSD of longitudinal velocity at 25 m $\bar{U} = 9.72\, m/s, \sigma_u = 1.03\, m/s,\ L_u = 50\, m$ Direction 73°MN, July 20th, 12:50 PM.

It turns out that although the two sequences correspond to the same wind direction with some comparable mean speed, their turbulence characteristics are found quite different. Especially the turbulence intensity is 15.1% versus 10.6% while the longitudinal turbulence scale is 168 m versus 50 m, leading to different PSD shapes.

4. PRESSURE DISTRIBUTION

4.1. Results with the motionless chimney

The wall pressures measured on the chimney at 26.75 m are presented. This altitude is at a distance 8.75 m (4.3 D) below the top and 11.75 m (5.9 D) upper the beginning of the diameter restriction. Therefore, one expects pressure distributions that should be close to those obtained with a 2D cylinder in a wind tunnel for high Reynolds flow regimes (Ellingsen et al. 2022c).

The time averaged pressure coefficients and the corresponding standard deviation are shown in Figure 8 for the first sequence.

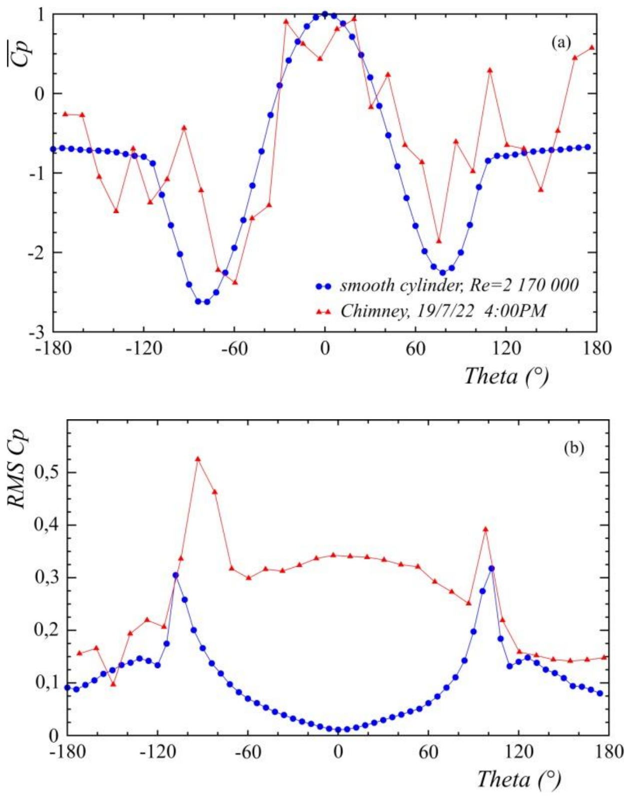

Figure 8. Time averaged (a) & standard deviation (b) of wall pressure coefficients distribution around the chimney at 26.75 m, July 19th 4:00 PM.

The pressure coefficient is defined as

$$Cp(\theta, t) = \frac{P(\theta,t) - P_{ref}}{\frac{1}{2}\rho \bar{U}^2} \quad \#(7)$$

where $P(\theta, t)$ is the instantaneous measured pressure at the azimuth angle θ. The reference pressure

P_{ref} is the mean static pressure inside the chimney and ρ is the air density corrected by atmospheric pressure and air temperature.

The azimuth angle θ=0° is referred to the wind direction as in a wind tunnel test section, so the present data in natural wind have been rotated in order to reach a “symmetrical” result which is of course imperfect due to the natural scatter of these observations. Note also that the spacing between taps is larger in the field experiments (11.25 °) than in the wind tunnel tests (6°).

Despite all, the results are satisfactory because the main characteristics of the pressure distribution can be detected, particularly the location and the value of the Cp_{min}. By comparison with wind tunnel data in smooth flow (Ellingsen et al. 2022c), it shows that the flow regime is clearly supercritical despite the disturbance generated by the atmospheric turbulence and shear.

Concerning the standard deviations, the two peaks around 100-110° observed in wind tunnel are also present in the field experiments. The high level of fluctuations in front of the chimney is due to the upstream turbulence which was, in contrast, very low in the wind tunnel.

4.2. Results with the oscillating chimney

In the sequence of July 20th at 12:45PM the chimney encountered oscillations which were visible to the naked eye. The motion was measured with the top accelerometers, leading to a standard deviation $\sigma_a = 2.09$ m/s^2 and a peak to peak value of ±3.62 m/s^2. The PSD shown in Figure 9 present clearly a peak of the oscillation frequency at 0.848 Hz, slightly lower than the first natural frequency measured during the manual excitation (0.868 Hz, see section 2.1).

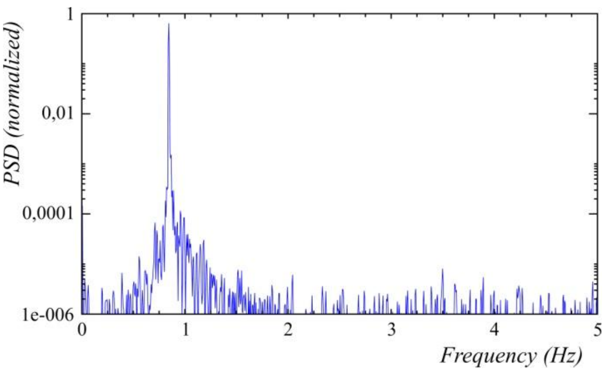

Figure 9. PSD of acceleration at the top, motion direction 43°MN $\sigma_a = 2.09\ m/s^2$ July 20th 12:45 PM

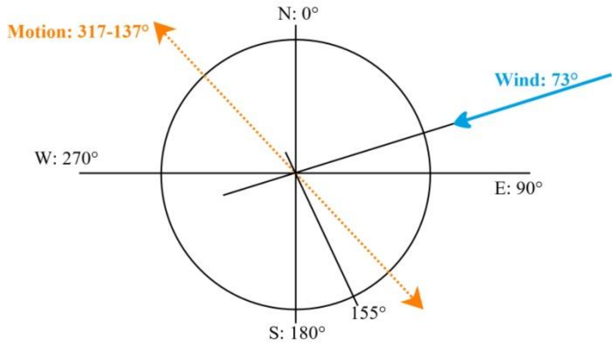

Figure 10. View in Magnetic North coordinate of the data from July 20th 12:45 PM.

From these data, the motion amplitude is estimated to be ± 0.128 m, which makes a peak to peak non dimensional amplitude of 0.128 D at the top. The direction of the motion, almost on a single axis, was measured and shown in the Figure 10. It appears that, in contrast to what could have been expected, the oscillations are not exactly normal to the mean wind direction, with an angle of 64° instead of the expected 90°. It might be the consequence of a memory effect of the flow or/and an inertial effect of the oscillating chimney from the past minutes prior the current observation.

The wall pressure distribution is presented in Figure 11. While it looks noisier, both mean values and fluctuating values are similar to the distribution observed the day before on the motionless chimney. It seems that the motion, which is after all not so large here, has no visible effect.

But more analysis and signal processing, such as bi-orthogonal decomposition (Hémon & Santi 2003), will be carried out in the near future.

Pressure taps along a vertical axis of the chimney are also available. Their angular position is 155° referred to magnetic North (see Figure 10) which is almost on the lateral right side relative to the wind direction. The correlation coefficient along this axis is shown Figure 12 for the two sequences of July the 19th on a motionless chimney and the 20th during oscillations. The reference location is taken at the top of the chimney. When the chimney is motionless, the correlation is surprisingly quite high, being still 0.24 at the distance 8.50 m (4.25 D). On the contrary, when the chimney oscillates, the correlation decreases more rapidly, down to 0.065 for the same distance.

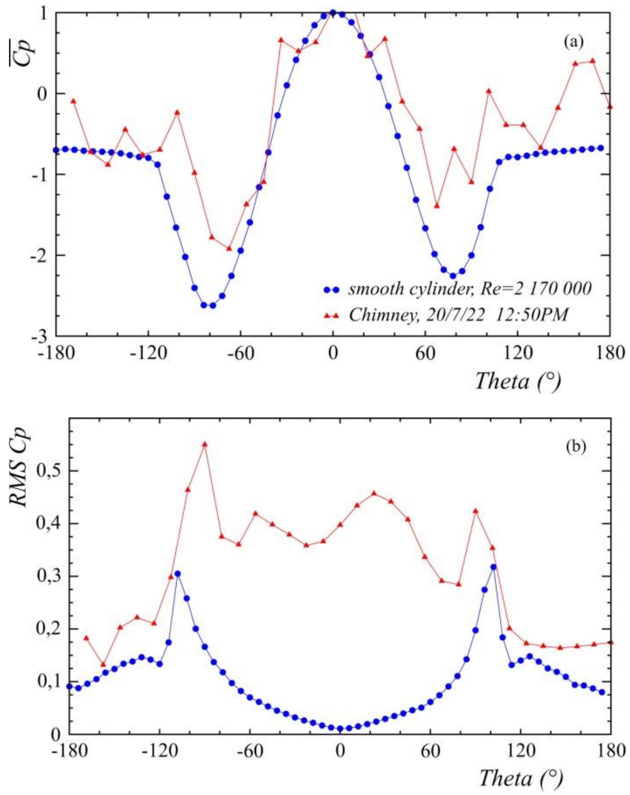

Figure 11. Time averaged (a) & standard deviation (b) of wall pressure coefficients distribution around the chimney at 26.75 m, July 20th 12:50 PM.

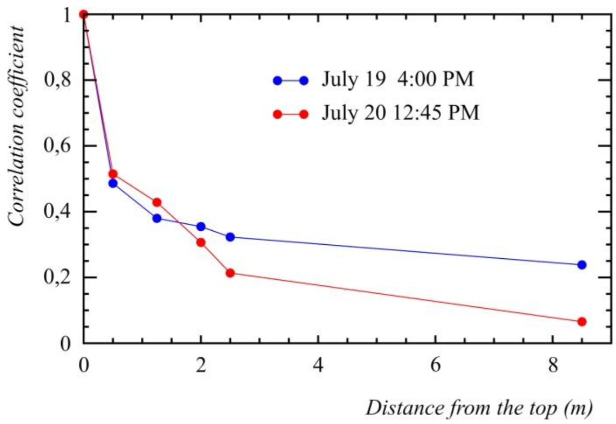

Figure 12. Correlation coefficient from the top (35.25 m) for pressure taps along the vertical axis at 155°MN, static chimney (July 19th) and oscillating (July 20th).

5. CONCLUSION

Unsteady wall pressure measurements have been performed on a full scale prototype chimney in natural wind. This experiment combines the two features that cannot be reproduced simultaneously in wind tunnel: a high Reynolds number and a turbulent boundary layer. Preliminary results have been presented, showing notably that the pressure distribution looks like the one measured in wind tunnel in supercritical conditions, with an additional turbulent noisy component.

More investigation are planned in the near future, especially signal processing using bi-orthogonal decomposition and Fourier analysis in order to better highlight the alternate vortex shedding in natural conditions.

6. ACKNOWLEDGEMENTS

This work is part of a partnership co-funded by Beirens (Poujoulat Group), Centre Scientifique et Technique du Bâtiment (CSTB), Centre National d'Etudes Spatiales (CNES) and LadHyX, CNRS-Ecole polytechnique.

Special acknowledgement is extended to Aurélien Jeanneton from Beirens for designing and constructing the chimney and to Olivier Flamand from CSTB for the measurement system operation.

7. REFERENCES

Barré, C. and Barnaud, G. 1995. High Reynolds number simulation techniques and their application to shaped structures model test. *J. Wind Eng. & Indus. Aerod.*, **57**, 145-157.

Basu RI, Vickery BJ. 1983 Across-wind vibrations of structure of circular cross-section. Part II. Development of a mathematical model for full-scale application. *J Wind Eng Ind Aerod.*;**12**(1), 75–97.

Christensen O, Askegaard V. 1978. Wind forces on and excitation of a 130-m concrete chimney. *J Wind Eng Ind Aerod.*, **3**(1), 61–77.

Ellingsen, Ø. M., Amandolese, X., Hémon, P., 2022a. In wind tunnel the reproduction of vortex shedding behind circular cylinder at high Reynolds number is incomplete. *Flow Induced Vibration*, FIV2022, Paris-Saclay, 5-8 July.

Ellingsen, Ø. M., Flamand, O., Amandolese, X., Coiffet, F., Hémon, P., 2022b. Field tests on a full-scale steel chimney subjected to vortex-induced vibrations. *Struct. Eng. Inter.*, **32**(1), 55-61.

Ellingsen, Ø. M., Amandolese, X., Flamand, O., Hémon, P., 2022c. Twin Strouhal numbers in pressure loading of circular cylinder at high Reynolds numbers. Submitted to *J. Fluids & Struct*.

European Committee for Standardization, 2005. Eurocode 1: Actions on structures - Part 1-4: General actions - Wind actions. Ref. n° EN 1991-1-4:2005 F.

Galemann T, Ruscheweyh H. 1992. Measurements of wind induced vibrations of a full-scale steel chimney. *J Wind Eng Ind Aerod.* ,**41**(1–3), 241–52.

Hémon, P., Santi, F., 2003. Applications of biorthogonal decompositions in fluid-structure interactions. *J. Fluids & Struct.,* **17.8**, 1123–1143.

Ruscheweyh H, Galemann T. 1996. Full-scale measurements of wind-induced oscillations of chimneys. *J Wind Eng Ind Aerod.*, **65**(1–3), 55–62.

Sageau, J.-F., 1978. Etude in situ du champ de pression stationnaire et instationnaire autour d'une cheminée de 240 m. *J. Wind Eng. & Indus. Aerod.*, **2**, 361–383.

Simiu, E., Scanlan, R., H., 1978. Wind effects on structures. An introduction to wind engineering. Wiley & Sons, New York.

Vickery BJ, Basu RI. 1983 Across-wind vibrations of structures of circular cross-section. Part I. Development of a mathematical model for two-dimensional conditions. J *Wind Eng Ind Aerod.* **12**(1), 49–73.